American Journal of Sciences and Engineering Research
E-ISSN -2348 – 703X, Volume 4, Issue 1, 2021

# Theoretical Investigation of the Molecular Structural Properties of Chloroquine, A Drug to Treat Coronavirus Disease 2019 through QTAIM, NBO, HOMO-LUMO Energies and Molecular Docking Modeling Studies

**Le Thi Thu Thuy[1], Lai Thi Hien[2], Bui Thi Phuong Thuy[3], Nguyen Ngoc Huong[4], Truong Tan Trung[5*]✉**

[1,2,4,5]*Dong Nai Technology University, Bien Hoa, Dong Nai 76000, Vietnam*
[3]*Van Lang University, Ho Chi Minh City, 700000, Vietnam*
*Corresponding author: truongtantrung@dntu.edu.vn*

**Abstract.** In this work, the molecular structures and vibrational spectra analysis of Chloroquine have been reported by Density Functional Theory calculations at B3LYP/6-311++G(2d,2p) level of theory. Intermolecular interactions were analyzed by AIM and NBO. Moreover, frontier molecular orbitals and molecular electrostatic potential (MEP) have been reported. Finally, using the molecular docking technique, molecular docking study was performed using MOE 2015.10. We report the inhibitory effect of the title compound on the host receptor angiotensin-converting enzyme 2 (ACE2) protein in the human body that leads to a crucial foundation about coronavirus resistance of title compounds on the main protease (PDB6LU7) protein of SARS-CoV-2. Results indicated that molecular docking simulation predicted the docking score (DS) > -10kcal.mol$^{-1}$ with significant intermolecular interaction at the catalytic triad or dyad (Arg 393, Phe 390, and Phe 40 of ACE2 protein; Cys 145, Phe 140, His 41, and Glu 166 of PDB6LU7 protein) and other essential substrate-binding residues of SARS-CoV-2 $M^{Pro}$. Therefore, Chloroquine may be considered to be a potent inhibitor of main protease protein SARS-CoV-2 but need to be explored for the further drug development process.

***Keywords:*** Chloroquine, Coronavirus, DFT, Molecular docking.

## I. INTRODUCTION

The World Health Organization (WHO) officially announced an acute respiratory infection (Covid-19) caused by a new strain of the corona virus (SARS-CoV-2) caused as a "global pandemic", in the context of the disease has spread to over 200 countries and territories. Since its first appearance in December 2019 in Wuhan City of Hubei Province, China and began spreading rapidly afterwards. As of June 7, 2020, there have been 6,750,521 confirmed cases of Covid-19, including 395,779 deaths. With increasing morbidity and mortality, scientists are trying to find drugs and vaccines to treat and prevent this disease. Several recent randomized trials have found some positive clinical effects and reduced mortality in the treatment with Lopinavir and Ritonavir [1].

Another drug recently tested in the treatment of Covid-19 is malaria meditcation : Chloroquine and its hydroxychloroquine derivatives. Because the previous In vitro studies have suggested that Chloroquine has activities that reduces the replication of diverse RNA / DNA viruses such as dengue virus [2], rabies virus [3], poliovirus [4], HIV virus [5], influenza A and B viruses [6], [7], influenza A $H_5N_1$ virus [8], Ebola virus [9], hepatitis B virus [10]. As for the SARS corona virus, there are also good signals in clinical experiments as a

strong inhibitor of infection and spread [11], which have demonstrated preliminary efficacy against corona virus concerned with SARS-CoV-2 [12], [13], [14]. However, the efficaciousness and safeness of Chloroquine in the therapeutic of SARS-CoV-2 still need to be clarified. To study the biosecurity and interactions between drugs and the biological goal is the use of molecular simulation methods [15], [16]. From this approach, it is possible to identify and quantify interactions between drugs and biological targets. Therefore, for the purpose of analyzing the structural, spectrum and electronic properties of Cholroquine as well as the interaction between Chloroquine and ACE2 (host of SARS-CoV-2) and protease PDB6LU7 (the main protease of SARS-CoV-2) [17], [18], along with some molecular chemical simulation techniques in used. We also compared the findings obtained in this study with some empirical datas , previously published works, such as oscillation frequency. The results of this study are considered a valuable document recommended for developing drugs or vaccines to prevent SARS-CoV-2 penertrating into the human body.

## II. COMPUTATIONAL METHODS

Quantum chemical calculations were carried out at the (Density Functional Theory-DFT) level using a hybrid functional B3LYP (Becke's three-parameter exchange functional [19] combined with the Lee-Yang-Parr correlation functional [20] with the 6-311++G(2d,2p) basis set [21]. Topological parameters such as electron density (ρ(rc)) and Laplacian of electron density ($\nabla^2$(ρ(rc)), electron kinetic energy density (G(rc)) and electron potential energy density (V(rc)) at bond critical points (BCP) of intermolecular interactions were identified using AIM2000 software [22] based on Bader's Atom in Molecules theory. The natural bond orbital (NBO) calculations were performed using GenNBO 5.G program as implemented in the Gaussian 09 package at the DFT/B3LYP/6-311++G(2d,2p) level [23]. In addition, molecular electrostatic potential (MEP) of title compound was investigated using theoretical calculations. All calculations were carried out using the GAUSSIAN 09 program [24]. The calculated results were visualized via the Gauss View program [25]. Finally, docking simulations of the interactions between title compound with the ACE2 and PDB6LU7 protein of SARS-CoV-2 was constructed using MOE 2015.10 software [26].

## III. RESULTS AND DISCUSSION

### 3.1. Quantum chemical calculations

*3.1.1. Geometric structure and topological analysis*

The molecular geometry optimization calculation was performed with the Gaussian 09 software package by using DFT method with B3LYP/6-311++G(2d,2p)) basis set. The optimized molecular structure of Chloroquine is display by GaussView software in Figure 1. The structure showed stable conformations and good structural with C1 symmetry. The global minimum energies energy values of Chloroquine (– 1326.33 a.u, B3LYP/6-311++G(2d,2p)) is close to the value previously reported by Noureddine et al. [27]. The C-N (C8-N17) bond length is 1.366 Å a shorter than the experimental value of 1.48 Å. Because resonance occurs in the C-N bond. Howere, The length of N-H bond (N17-H18, 1.004 Å) is longer that the experimental value of 0.840 Å.

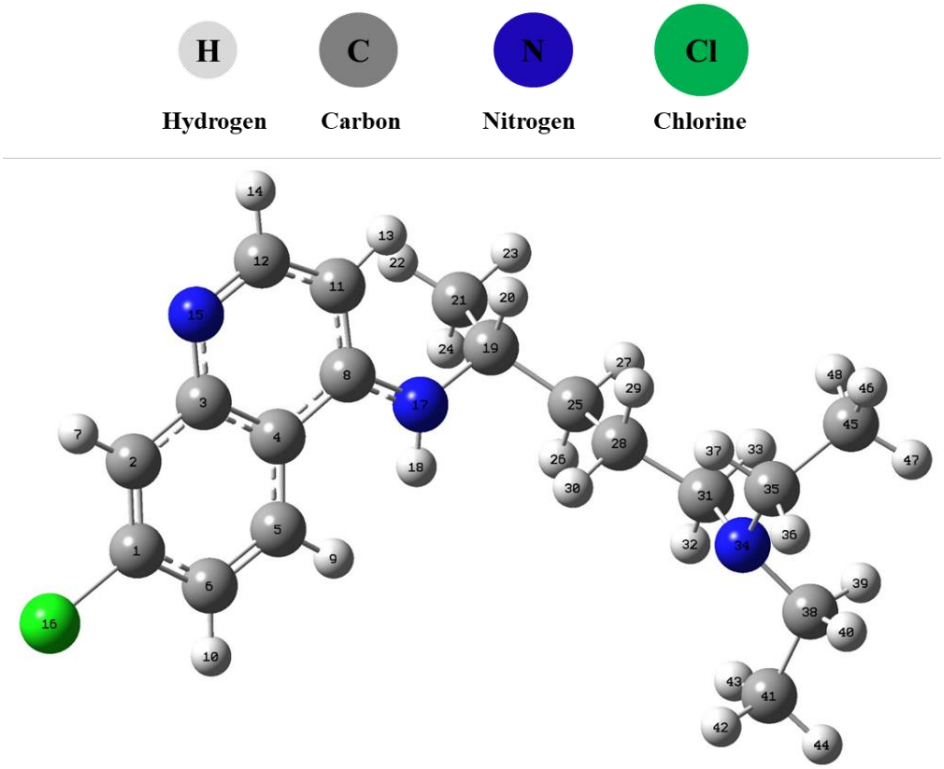


**Figure 1:** The optimized molecular structure and atom numbering scheme adopted for Chloroquine at the B3LYP/6-311++G(2d,2p) level

Atom in molecules (AIM) theory by Bader [28], [29] is used analysis the strength of various interactions and bonding existing in the compound. Electron kinetic energy density (G(rc)) and electron potential energy density (V(rc)) at the bond critical points (BCP) are related to each other via the formula:

$$¼ \nabla^2\rho(rc) = 2G(rc) + V(rc) \quad (1)$$

The total electron energy density at BCP depends on the balance between (G(rc)) and (V(rc)) is calculated by:

$$H(rc) = G(rc) + V(rc) \quad (2)$$

On the basis of AIM analysis, energy of each HB is calcuated using the formula [30], [31]

$$E_{HB} = 0{,}5V(rc) \quad (3)$$

The results from AIM analysis are given in Table 1 also shows all the values of ρ(rc), Laplacian $\nabla^2\rho(rc)$ at the BCP in the ranges of 0.1878 a.u – 0.3611 a.u. These values fall within the critical limit for formation of co-valent interactions as indicated by $\nabla^2\rho(rc) < 0$, $H(rc) < 0$, and $G/|V(rc)| > 1$ [32], except for the BCP of N17 - H18···C5 - H9 with values of Laplacian $\nabla^2\rho(rc) > 0$ (0.0525 a.u), $H(rc) > 0$ (0.0022 a.u), and $G/|V(rc)| > 1$ (1.256). These values fall within the critical limit for formation of weak interactions [33]. In table 1, N15-C12 (N17-H8) has high electron density (0.3611, 0.3526 a.u, respectively), Laplacian of the electron density (-1.1764 a.u, -1.7500 a.u). It shows that the bond has the highly donating nature of electrons. The values of energy each HB ($E_{HB}$ = -11.408 kcal.mol$^{-1}$, N17 - H18···C5 - H9) is very low. So that, All the bond in title compound has high bond energy that leads to co-valent bond type, except N17 - H18···C5 - H9 inteactions. In addition, there are four ring critical point (RCP), two in the middle of the aromatic ring and two between the H20 (H18) on C19-H20 (N17-H18) and H13 (H9) aromatic ring, respectively.

**Table 1:** Selected parameters at the BCP of bond interactions for Chloroquine by AIM analysis

| Bond | ρ(r) | $\nabla^2\rho(r)$ | G(r)[a)] | V(r)[b)] | G/\|V(r)\| | H(r)[c)] | $E_{HB}$[d)] |
|---|---|---|---|---|---|---|---|
| | (a.u.) | (a.u.) | (a.u.) | (a.u.) | | (a.u.) | (Kcal.mol$^{-1}$) |
| N17 - H18···C5 - H9 | 0.0137 | 0.0525 | 0.0109 | -0.0087 | 1.256 | 0.0022 | -11.408 |
| C6 - H10 | 0.2920 | -1.1035 | 0.0391 | -0.3541 | 0.110 | -0.3150 | -464.843 |
| C1 - Cl16 | 0.1878 | -0.2098 | 0.0636 | -0.1797 | 0.354 | -0.1160 | -235.840 |
| C2 - H7 | 0.2928 | -1.1132 | 0.0373 | -0.3529 | 0.106 | -0.3156 | -463.241 |
| C12 - H14 | 0.2932 | -1.1160 | 0.0356 | -0.3501 | 0.102 | -0.3146 | -459.611 |
| C11 - H13 | 0.2896 | -1.0755 | 0.0440 | -0.3568 | 0.123 | -0.3129 | -468.428 |
| N15 - C3 | 0.3304 | -1.0044 | 0.1533 | -0.5576 | 0.275 | -0.4044 | -732.044 |
| N15 - C12 | 0.3611 | -1.1764 | 0.2264 | -0.7469 | 0.303 | -0.5205 | -980.522 |
| N17 - C19 | 0.2573 | -0.6601 | 0.1095 | -0.3840 | 0.285 | -0.2745 | -504.126 |
| N17 - C8 | 0.3172 | -0.9911 | 0.1682 | -0.5841 | 0.288 | -0.4159 | -766.781 |
| N34 - C35 | 0.2623 | -0.6258 | 0.0975 | -0.3514 | 0.277 | -0.2539 | -461.275 |
| N17 - H8 | 0.3526 | -1.7500 | 0.0629 | -0.5632 | 0.112 | -0.5004 | -739.347 |
| C21 - H20 | 0.2893 | -1.0651 | 0.0409 | -0.3481 | 0.118 | -0.3072 | -457.019 |
| C21 - H22 | 0.2830 | -1.0229 | 0.0441 | -0.3439 | 0.128 | -0.2998 | -451.412 |
| C21 - H23 | 0.2806 | -1.0063 | 0.0448 | -0.3412 | 0.131 | -0.2964 | -447.848 |
| C21 - H24 | 0.2803 | -1.0028 | 0.0450 | -0.3407 | 0.132 | -0.2957 | -447.201 |
| C25 - H26 | 0.2785 | -0.9851 | 0.0457 | -0.3377 | 0.135 | -0.2920 | -443.358 |
| C25 - H27 | 0.2823 | -1.0136 | 0.0447 | -0.3428 | 0.130 | -0.2981 | -450.059 |
| C28 - H29 | 0.2820 | -1.0102 | 0.0458 | -0.3442 | 0.133 | -0.2984 | -451.860 |
| C28 - H30 | 0.2843 | -1.0275 | 0.0438 | -0.3445 | 0.127 | -0.3007 | -452.261 |
| C31 - H32 | 0.2876 | -1.0533 | 0.0429 | -0.3490 | 0.123 | -0.3062 | -458.174 |
| C31 - H33 | 0.2776 | -0.9765 | 0.0429 | -0.3298 | 0.130 | -0.2870 | -433.002 |
| C35 - H36 | 0.2868 | -1.0504 | 0.0418 | -0.3462 | 0.121 | -0.3044 | -454.427 |
| C35 - H37 | 0.2880 | -1.0587 | 0.0419 | -0.3484 | 0.120 | -0.3066 | -457.418 |
| C38 - H39 | 0.2791 | -0.9887 | 0.0423 | -0.3318 | 0.128 | -0.2895 | -435.562 |
| C38 - H40 | 0.2871 | -1.0525 | 0.0420 | -0.3472 | 0.121 | -0.3051 | -455.728 |
| C41 - H42 | 0.2811 | -1.0082 | 0.0459 | -0.3439 | 0.134 | -0.2980 | -451.425 |
| C41 - H43 | 0.2822 | -1.0174 | 0.0441 | -0.3425 | 0.129 | -0.2984 | -449.578 |
| C41 - H44 | 0.2800 | -1.0025 | 0.0451 | -0.3408 | 0.132 | -0.2957 | -447.389 |
| C45- H46 | 0.2796 | -0.9980 | 0.0456 | -0.3407 | 0.134 | -0.2951 | -447.199 |
| C45 - H47 | 0.2809 | -1.0067 | 0.0455 | -0.3427 | 0.133 | -0.2972 | -449.856 |
| C45 - H48 | 0.2806 | -1.0044 | 0.0459 | -0.3430 | 0.134 | -0.2970 | -450.213 |

*3.1.2. Natural bond orbital analysis*

The secon-order perturbation theory is stuied intra and inter-molecular non bond interactions for molecular compound. The second-order Fock matrix was carried out to evaluate the donor → acceptor interactions in NBO analysis [34]. The second-order perturbation interaction energy ($E^{(2)}$) is calcuated using the formula [35], [36], [37], [38]:

$$E^{(2)} = \Delta E_{\mathrm{ij}} = q_{\mathrm{i}} \frac{F_{\mathrm{ij}}^2}{\varepsilon_j - \varepsilon_i}$$

Where $q_i$ is the occupancy of donor orbital, $\varepsilon_i$ and $\varepsilon_j$ are diagonal elements and F(i,j) is the off-diagonal Fock matrix element. NBO analysis was performed on the Chloroquine at the DFT/B3LYP/6-311++G(2d,2p) level and the results are presented in Table 2.

The NBO analysis (Table 2) for the Chloroquine molecule revealed strong the energy of hyper conjugative interaction of LP → $\pi^*$ transitions that lead to an intramolecular electronic density transfer. The presence of electron transfer processes from n(N) to σ*(C−C) and σ*(C-H) anti-bonding orbitals, the (E(2)) associated with hyperconjugative interaction of LP(N15) → σ*(C3-C4), LP(N15) → σ*(C11-C12), and LP(N15) → σ*(C12-H14) were respectively 10.13 Kcal/mol, 9.6 Kcal/mol and 4.37 Kcal/mol. Moreover, LP(N17) → σ*(C8-C11), σ*(C19-C21) were espectively 47.95 and 7.19 Kcal/mol; LP(N34) → σ*(C31-H33) (E(2) = 9.29 Kcal/mol), σ*(C35-H39) (E(2) = 8.33 Kcal/mol) and σ*(C35-C45) (E(2) = 8.57 Kcal/mol). These results will be analyzed more clearly in the molecular electrostatic potential.

**Table 2:** Second-order perturbation theory anlaysis of the Fock matrix in NBO donor-acceptor

| Donor NBO (i) | **Type** | Aceeptor NBO (j) | **Type** | **$E^{(2)}$ [a]** | **E(j)-E(i) [b]** | **F(i,j) [c]** |
|---|---|---|---|---|---|---|
| | | | | Kcal/mol | a.u. | a.u. |
| N15 | LP | C3-C4 | σ* | 10.13 | 0.85 | 0.084 |
| N15 | LP | C11-C12 | σ* | 9.60 | 0.91 | 0.085 |
| N15 | LP | C12-H14 | σ* | 4.37 | 0.78 | 0.053 |
| N17 | LP | C8-C11 | σ* | 47.95 | 0.29 | 0.108 |
| N17 | LP | C19-C21 | σ* | 7.19 | 0.62 | 0.064 |
| N34 | LP | C31-H33 | σ* | 9.29 | 0.66 | 0.072 |
| N34 | LP | C35-C45 | σ* | 8.57 | 0.63 | 0.067 |
| N34 | LP | C38-H39 | σ* | 8.33 | 0.67 | 0.068 |

[a] $E^{(2)}$ means the energy of hyper conjugative interaction
[b] Energy difference between Donor (i) and Aceeptor (j)
[c] F(i,j) the off-diagonal NBO Fock matrix element

*3.1.3. Frontire molecular orbitals and molecular electrostatic potential*

The highest occupied molecular orbital (HOMO) and lowest unoccupied molecular orbital (LUMO). HOMO represents the donor of an electron and LUMO represents the acceptor of an electron. HOMO and LUMO are the two most important molecular orbitals in a molecule as both are used to describe various chemical properties such as reactivity and kinetics. The diagrams of $\Delta E_{HOMO\text{-}LUMO}$ energy are shown in Figure 2a. The calculated values of HOMO and LUMO energy are -5.94 eV, -1.55 eV respectively. The $\Delta E_{HOMO\text{-}LUMO}$ energy gap value is predicted 4.39 eV that explains the ultimate transfer fo charge happeing within the molecule, which influences the biological activity of the Chloroquine.

The Molecular Electrostatic Potential (MEP) which is a plot of electrostatic potential mapped into the constant electron density surface. The importance of MEP lies in the fact that it displays molecular shape, size, and electrostratic potential in terms of color. Figure 2b shows the MEP plot for the title compound calcuated by DFT/B3LYP method with 6-311++G(2d,2p) basis set using the computer software GaussView. The different values of the electrostatic potential at the surface are represented by different colors. The negative region are represented by red, blue represented the regions of the positive potential and the green represents the region of zero potential. From the MEP, the negative regions (red color) are mainly near the N15 and N34 atoms; the positive (bule color) is around the H18 atom. These two sites are associated with electrophilic and nucleophin reactivity, which the evidence of the biological actibity of the Chloroquine. This assignment will be verified from molecular modeling study below.

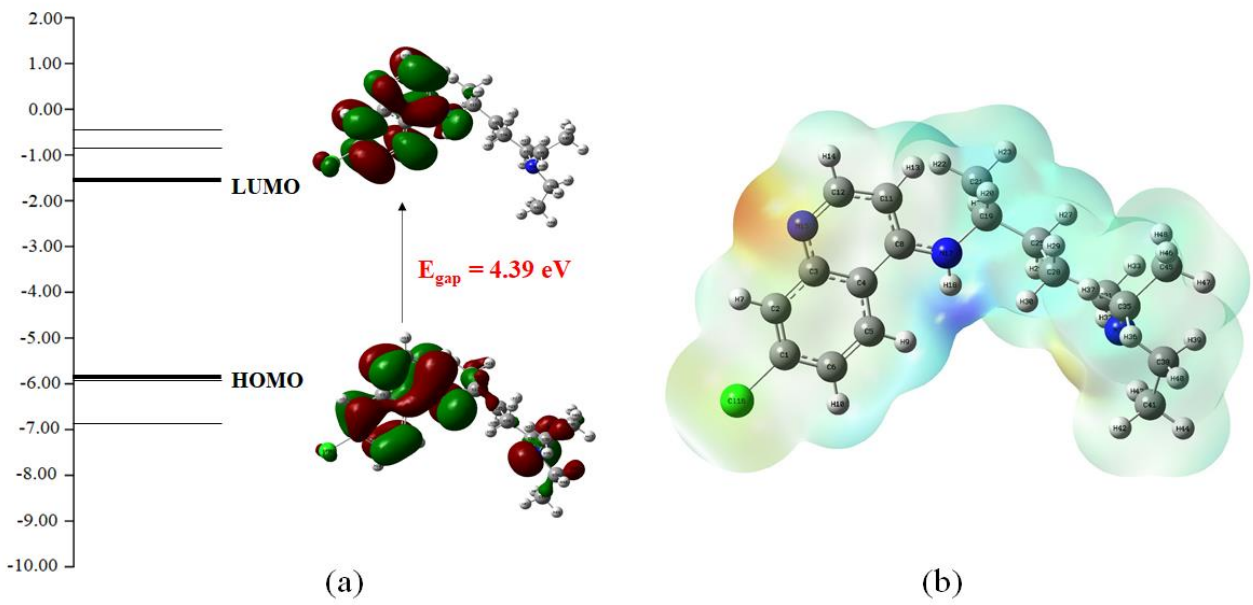


**Figure 2:** (a) The $\Delta E_{HOMO-LUMO}$ energy gap and (b) Molecular Electrostatic Potential (MEP) map for Chloroquine calculated by DFT methods at the B3LYP/6-311++G(2d,2p) level.

### 3.2. Molecular modeling study

Downloading the ACE2 (code Q9BYF1) and PDB6LU7 [17], [18] using MOE 2015.10 [26]. Docking Chloroquine to ACE2 and PDB6LU7 compex using Triangle Matching method, the number of poses to keep for further analysis of interaction is 10. The maximum number of solution per iteration is 1000. The maximum number of solutions per fragmentation is 200. The best result of model structure is evaluated by root mean square deviation (RMSA, Å) and the most minus docking score (DS, kcal.mol$^{-1}$) with number of interactions and type of interaction.

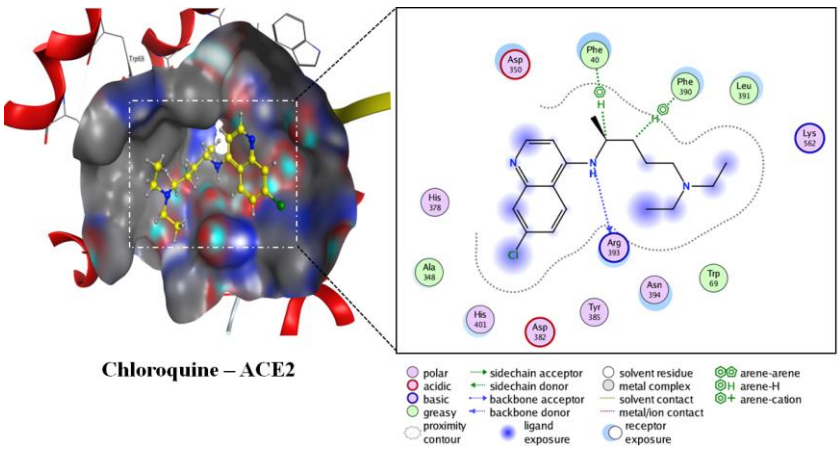


| Chloroquine | | ACE2 | Interaction | Distance | E | DS | RMSD |
|---|---|---|---|---|---|---|---|
| N 17 | O | Arg 393 | H-donor | 3.48 | -0.6 | | |
| C25 | 6-ring | Phe 390 | H-pi | 4.21 | -0.7 | -10.388 | 1.351 |
| C19 | 6-ring | Phe 40 | H-pi | 4.69 | -0.7 | | |

**Figure 3**. Interactions between the Chloroquine compound with enzyme ACE2

Conducting docking in to ACE2, PDB6LU7 protenin, results are shown in Figure 3 and Figure 4. Hydrogen bonds,, cation-π, π-π bond, ionic and van der Waals interaction of Chloroquiner and ACE2, PDB6LUP7 protein were also analyzed using MOE 2015.10 (Figure 3 and Figure 4). The simulation results

showed that Chloroquine has the best interaction with ACE2: inclusing the H-donor interaction between N17 with Oxy of Arg 393; the H-π interaction between C25 and C19 with 6-ring of Phe 390, Phe 40 respectively with the lowest docking score (DS) and smallest distance: DS = -10.388 kcal.mol$^{-1}$; root mean square deviation (RMSD) = 1.351 Å. Chloroquine has N34, Cl16, C21, 6-ring group interacting H-donor and H-π with SG, O, 5-ring, and N of Cys 145, Phe 140, His 41, and Glu 166 of PDB6LU7 protein; with DS = -11.169 kcal.mol-; RMSD = 1.084 Å. The results of docking simulation showed that Chloroquine has the ability to inhibit SARS-Cov-2.

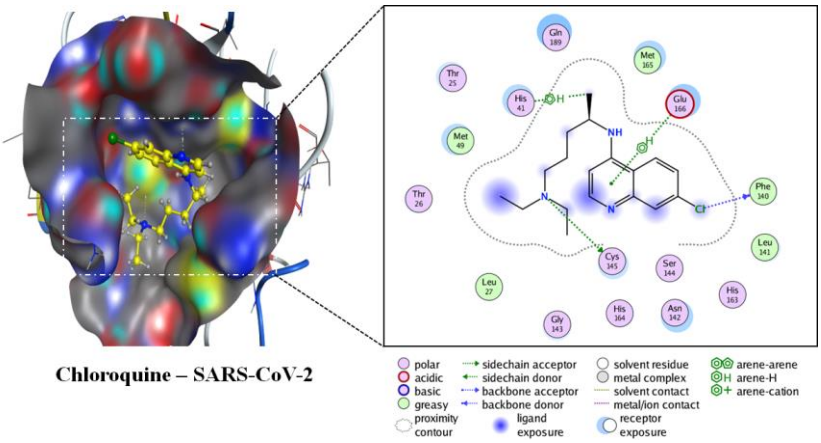


| Chloroquine | PDB6LU7 | | Interaction | Distance | E | DS | RMSD (Å) |
|---|---|---|---|---|---|---|---|
| N34 | SG | Cys 145 | H-donor | 3.92 | -1.4 | -11.619 | 1.084 |
| Cl16 | O | Phe 140 | H-donor | 3.16 | -0.1 | | |
| C21 | 5-ring | His 41 | H-pi | 3.79 | -0.7 | | |
| N | 6-ring | Glu 166 | pi-H | 3.94 | -0.8 | | |

**Figure 4**. Interactions between the Chloroquine compound with enzyme PDB6LU7

## IV. CONCLUSIONS

In this work, quantum chemical calculations on energy and molecular structure of Chloroquine has been attempted by implementing DFT/B3LYP method using 6-311++G(2d,2p) basis sets. The topological parameters were analyzed using the atoms in molecules (AIM) theory using the AIM 2000 package. Moreover, the donating tendency from electron donors to electron acceptors about intermolecular charge transfer were analyzed by NBO. The $\Delta E_{HOMO\text{-}LUMO}$ energy is calculated to be 4.39 eV, which suggestions the biological activity of the Chloroquine compound. The MEP map shows the negative potential sites are on N15 atoms and N34, as well as the positive potential sites, are around the H18. Based on the docking score, Chloroquine can be used as a potential SARS-Cov-2 $M^{pro}$ inhibitor. However, further studies are needed to validate the antiviral properties of the Chloroquine drug against SARS-Cov-2 $M^{pro}$.

## V. ACKNOWLEDGMENTS

The author is grateful to Ph.D student Nguyen Thanh Si, Can Tho University for all kind of supporting the Gaussian 09 program.

## VI. REFERENCES

[1] B. Cao *et al.*, "A trial of lopinavir–ritonavir in adults hospitalized with severe Covid-19," *New England Journal of Medicine,* 2020.

[2] K. J. S. Farias, P. R. L. Machado, R. F. de Almeida Junior, A. A. de Aquino, and B. A. L. da Fonseca, "Chloroquine interferes with dengue-2 virus replication in U937 cells," *Microbiology and immunology,* vol. 58, no. 6, pp. 318-326, 2014.

[3] H. Tsiang and F. Superti, "Ammonium chloride and chloroquine inhibit rabies virus infection in neuroblastoma cells," *Archives of virology,* vol. 81, no. 3-4, pp. 377-382, 1984.

[4] P. Kronenberger, R. Vrijsen, and A. Boeyé, "Chloroquine induces empty capsid formation during poliovirus eclipse," *Journal of virology,* vol. 65, no. 12, pp. 7008-7011, 1991.

[5] F. Romanelli, K. M. Smith, and A. D. Hoven, "Chloroquine and hydroxychloroquine as inhibitors of human immunodeficiency virus (HIV-1) activity," *Current pharmaceutical design,* vol. 10, no. 21, pp. 2643-2648, 2004.
[6] E. E. Ooi, J. S. W. Chew, J. P. Loh, and R. C. Chua, "In vitro inhibition of human influenza A virus replication by chloroquine," *Virology journal,* vol. 3, no. 1, p. 39, 2006.
[7] M. Shibata *et al.*, "Mechanism of uncoating of influenza B virus in MDCK cells: action of chloroquine," *Journal of General Virology,* vol. 64, no. 5, pp. 1149-1156, 1983.
[8] Y. Yan *et al.*, "Anti-malaria drug chloroquine is highly effective in treating avian influenza A H5N1 virus infection in an animal model," *Cell research,* vol. 23, no. 2, pp. 300-302, 2013.
[9] S. D. Dowall *et al.*, "Chloroquine inhibited Ebola virus replication in vitro but failed to protect against infection and disease in the in vivo guinea pig model," *The Journal of general virology,* vol. 96, no. Pt 12, p. 3484, 2015.
[10] E. Kouroumalis and J. Koskinas, "Treatment of chronic active hepatitis B (CAH B) with chloroquine: a preliminary report," *Annals of the Academy of Medicine, Singapore,* vol. 15, no. 2, pp. 149-152, 1986.
[11] M. J. Vincent *et al.*, "Chloroquine is a potent inhibitor of SARS coronavirus infection and spread," *Virology journal,* vol. 2, no. 1, p. 69, 2005.
[12] A. Savarino, J. R. Boelaert, A. Cassone, G. Majori, and R. Cauda, "Effects of chloroquine on viral infections: an old drug against today's diseases," *The Lancet infectious diseases,* vol. 3, no. 11, pp. 722-727, 2003.
[13] P. Colson, J.-M. Rolain, and D. Raoult, "Chloroquine for the 2019 novel coronavirus," *Int J Antimicrob Agents,* 2020.
[14] C. A. Devaux, J.-M. Rolain, P. Colson, and D. Raoult, "New insights on the antiviral effects of chloroquine against coronavirus: what to expect for COVID-19?," *International Journal of Antimicrobial Agents,* p. 105938, 2020.
[15] J. H. Shibata, "Review of molecular modeling basics," ed: ACS Publications, 2012.
[16] G. B. Barcellos *et al.*, "Molecular modeling as a tool for drug discovery," *Current drug targets,* vol. 9, no. 12, pp. 1084-1091, 2008.
[17] Z. Jin *et al.*, "Structure of Mpro from COVID-19 virus and discovery of its inhibitors," *bioRxiv,* 2020.
[18] X. Liu, B. Zhang, Z. Jin, H. Yang, and Z. Rao, "The crystal structure of COVID-19 main protease in complex with an inhibitor N3," ed, 2020.
[19] A. D. Becke, "Density-functional exchange-energy approximation with correct asymptotic behavior," *Physical review A,* vol. 38, no. 6, p. 3098, 1988.
[20] C. Lee, W. Yang, and R. G. Parr, "Development of the Colle-Salvetti correlation-energy formula into a functional of the electron density," *Physical review B,* vol. 37, no. 2, p. 785, 1988.
[21] R. A. Kendall, T. H. Dunning Jr, and R. J. Harrison, "Electron affinities of the first-row atoms revisited. Systematic basis sets and wave functions," *The Journal of chemical physics,* vol. 96, no. 9, pp. 6796-6806, 1992.
[22] F. Biegler-König, D. Bayles, and J. Schönbohm, "AIM 2000 1.0," *University of Applied Sciences: Bielefeld, Germany,* 2000.
[23] E. Glendening *et al.*, "Theoretical chemistry institute," *University of Wisconsin, Madison,* 2001.
[24] M. Frisch *et al.*, "Gaussian 09 Revision D. 01, 2009, Gaussian Inc," *Wallingford CT,* vol. 93, 2009.
[25] R. Dennington, T. Keith, and J. Millam, "Semichem Inc," *Shawnee Mission KS, GaussView, Version,* vol. 5, 2009.
[26] Chemical Computing Group Inc., "MOE (The Molecular Operating Environment), 1010 Sherbrooke Street West, Suite 910, Montreal, Canada H3A 2R7. http://www.chemcomp.com.
," 2015.
[27] O. Noureddine, N. Issaoui, and O. J. J. o. K. S. U.-S. Al-Dossary, "DFT and molecular docking study of chloroquine derivatives as antiviral to coronavirus COVID-19," vol. 33, no. 1, p. 101248, 2020.
[28] R. F. Bader, "Atoms in molecules," *Accounts of Chemical Research,* vol. 18, no. 1, pp. 9-15, 1985.
[29] R. Bader, "AIMPAC: a suite of programs for the theory of atoms in molecules, Hamilton, Canada (contact http://www. chemistry. mcmaster. ca/aimpac) Search PubMed; RFW Bader, Atoms in Molecules: A Quantum Theory," ed: Clarendon Press, Oxford, 1990.
[30] E. Espinosa, E. Molins, and C. Lecomte, "Hydrogen bond strengths revealed by topological analyses of experimentally observed electron densities," *Chemical physics letters,* vol. 285, no. 3-4, pp. 170-173, 1998.

[31] I. Mata, I. Alkorta, E. Espinosa, and E. Molins, "Relationships between interaction energy, intermolecular distance and electron density properties in hydrogen bonded complexes under external electric fields," *Chemical Physics Letters,* vol. 507, no. 1-3, pp. 185-189, 2011.

[32] P. S. V. Kumar, V. Raghavendra, and V. Subramanian, "Bader's theory of atoms in molecules (AIM) and its applications to chemical bonding," *Journal of Chemical Sciences,* vol. 128, no. 10, pp. 1527-1536, 2016.

[33] M. Ziółkowski, S. J. Grabowski, and J. Leszczynski, "Cooperativity in hydrogen-bonded interactions: ab initio and "atoms in molecules" analyses," *The Journal of Physical Chemistry A,* vol. 110, no. 20, pp. 6514-6521, 2006.

[34] A. E. Reed, L. A. Curtiss, and F. Weinhold, "Intermolecular interactions from a natural bond orbital, donor-acceptor viewpoint," *Chemical Reviews,* vol. 88, no. 6, pp. 899-926, 1988.

[35] A. E. Reed and F. Weinhold, "Natural bond orbital analysis of near-Hartree–Fock water dimer," *The Journal of chemical physics,* vol. 78, no. 6, pp. 4066-4073, 1983.

[36] A. E. Reed and F. Weinhold, "Natural localized molecular orbitals," *The Journal of chemical physics,* vol. 83, no. 4, pp. 1736-1740, 1985.

[37] A. E. Reed, R. B. Weinstock, and F. Weinhold, "Natural population analysis," *The Journal of Chemical Physics,* vol. 83, no. 2, pp. 735-746, 1985.

[38] a. J. Foster and F. Weinhold, "Natural hybrid orbitals," *Journal of the American Chemical Society,* vol. 102, no. 24, pp. 7211-7218, 1980.